

## Swirl Atomizers with Coanda Deflection Outlets

E. Musemic<sup>\*</sup>, P. Walzel

Department of Biochemical Engineering, Technische Universität Dortmund, Germany  
emir.musemic@bci.tu-dortmund.de and peter.walzel@bci.tu-dortmund.de

### Abstract

Swirl Atomizers are used in a wide range of technical applications. From what is known from the literature, the mean drop size decreases with increasing spray angle. A method to increase the spray angle, apart from intensifying the swirl, is to provide the nozzle outlet with trumpet openings. The attached film flow follows the contour due to the Coanda effect. Although such nozzles are already part of the product line for most of the nozzle manufacturers, the understanding of the Coanda-effect for two-phase flows is still missing. In the present paper this effect was analyzed experimentally in order to observe the general deflection behavior at swirl atomizers and to provide additional insight into the mechanism for the two-phase flow. It was observed, that higher Reynolds-numbers lead to an earlier sheet detachment. The wetting angle of the nozzle material was found to have no influence on the deflection behavior, indicating that the “tea pot effect” is not significant within the considered operational area. The ambient gas pressure has a noticeable impact on the detachment behavior, as higher ambient pressures promote a premature sheet detachment, while the atomization differential pressure is kept constant.

---

### Introduction

Swirl Atomizers are used in a wide range of technical applications, due to their good atomization performance and plugging insensibility. The field of application includes spray drying in the chemical industry, fuel combustion, agricultural spraying and many others. The nozzle sizes and insert geometries vary from application to application within wide ranges, although the basic atomization concept is identical. The liquid usually enters the spin chamber tangentially, either through one or multiple tangential oriented inlets or through a swirl body with multiple grooves. In this way, a swirl flow is imposed, with the tangential velocity increasing for  $r \rightarrow 0$  and the local liquid pressure decreasing accordingly. At a certain radial position, the local liquid pressure reaches the ambient gas pressure, leading to air entrainment into the nozzle center. Thus a nearly cylindrical air core is formed, occupying a part of the nozzle outlet cross section. Therefore, the liquid emerges from the orifice as a liquid sheet, which follows divergent straight trajectories as a consequence of the swirl flow inside the nozzle

The subsequent sheet break up is taking place due to different break-up mechanisms [1], either dominated by the aerodynamically induced flapping motion or by turbulent break-up. The first takes place at moderate liquid pressures, the ambient gas leading to growth of initial disturbances along the streamlines. At a certain location the sheet thickness reaches the critical value and the sheet breaks up into fragments. The size of the fragments can be linked to the sheet oscillation wavelength [2,3] and to the resulting drop sizes, as the fragments contract to threads, which later on resolve to droplets. The advantage of atomization within the aerodynamically induced break-up regime is the relatively narrow drop size distribution and the mean drop size is small compared to the nozzle orifice diameter at the same time. These advantages make this operating regime especially suitable for the production of granular material through spray drying. The relatively moderate drop velocities obtained here may also be desired e.g. in agricultural applications. With increasing flow velocities, the turbulent break-up is gradually coming up and the break-up location of the liquid sheet moves towards the nozzle orifice. The mean drop size decreases compared to aerodynamically induced break-up, while the distribution width increases significantly. The intensive mixing of liquid and gas is typical for the turbulent regime, which makes it especially interesting for fuel combustion applications.

In the present work, the focus lies on the aerodynamically induced break-up. For low viscosity of the sprayed fluids, the mean drop size can be estimated with a relationship by Dombrowski and Johns [2]:

$$\frac{SMD}{D} = 1,3 \cdot \left( \frac{\kappa}{2 \varphi^2 \Delta p^*} \right)^{1/3} \left( \frac{\rho_l}{\rho_g} \right)^{1/6} \quad (1)$$

---

\* Corresponding author: emir.musemic@bci.tu-dortmund.de

Here,  $\varphi$  is the velocity coefficient with  $\varphi = w_{\text{eff}}/w_{\text{pot}}$  and  $\Delta p^*$  the Laplace-number with  $\Delta p^* = \Delta p_l D / \sigma$ , with the orifice diameter as the characteristic length.  $\kappa$  is the sheet number, which considers the sheet thinning effect due to the divergent liquid flow, describing the local sheet thickness  $\delta/D$  as a function of the relative distance from the orifice  $x/D$ :

$$\kappa = \frac{\delta x}{A_D} = \frac{C_D}{2 \pi \varphi \sin(\Theta/2)} \quad (2)$$

$\delta x$  also was defined as sheet parameter in [2].  $C_D$  is the discharge coefficient, defined as the ratio of the average axial velocity at the nozzle outlet to the potential velocity obtained with the atomization pressure  $\Delta p_l$ :

$$C_D = \frac{\bar{v}}{A_D} \sqrt{\frac{\rho_l}{2 \Delta p_l}} \quad (3)$$

As shown in eq. (2), the sheet number  $\kappa$  strongly depends on the discharge coefficient  $C_D$  and the spray angle  $\Theta$ . Both parameters depend on the intensity of the swirl flow inside the nozzle, as higher tangential velocities produce thinner sheets and wider spray angles. The values for  $C_D$ ,  $\varphi$  and  $\Theta$  can be either obtained experimentally or be estimated with correlations presented in [1], [4], and [5]. The swirl flow intensity inside the nozzle can be described with the swirl ratio  $\Delta$ , as shown in [6].

The swirl ratio is defined by relating the theoretical tangential velocity  $u$  at the nozzle outlet to the average axial velocity  $\bar{v}$ , where the effective axial velocity  $v$  is averaged for the whole outlet cross section. By neglecting the energy losses due to friction and turbulence effects, the swirl ratio can be expressed with the nozzle geometry only, as shown in eq. (4).

$$\Delta = \frac{u}{\bar{v}} = \frac{\pi r_{SC,E} D}{2 A_E} \quad (4)$$

In eq. (4),  $r_{SC,E}$  is the swirl chamber radius of the tangential liquid inlet, while  $A_E$  is the total inlet flow cross section. Common swirl nozzle designs reach  $\Delta$ -values between 1 and 8. Higher swirl ratios cause higher spray angles, as well as lower discharge coefficients.

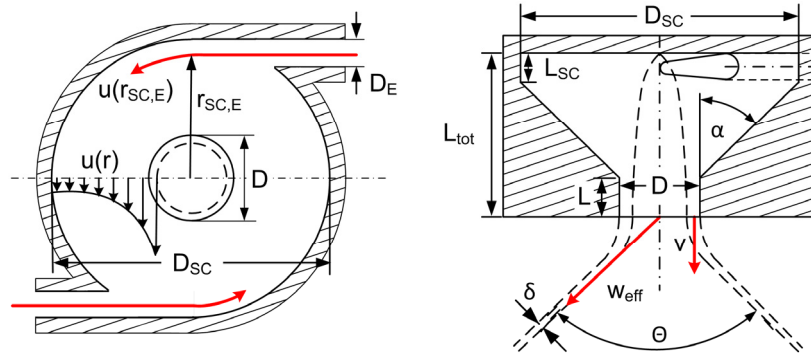
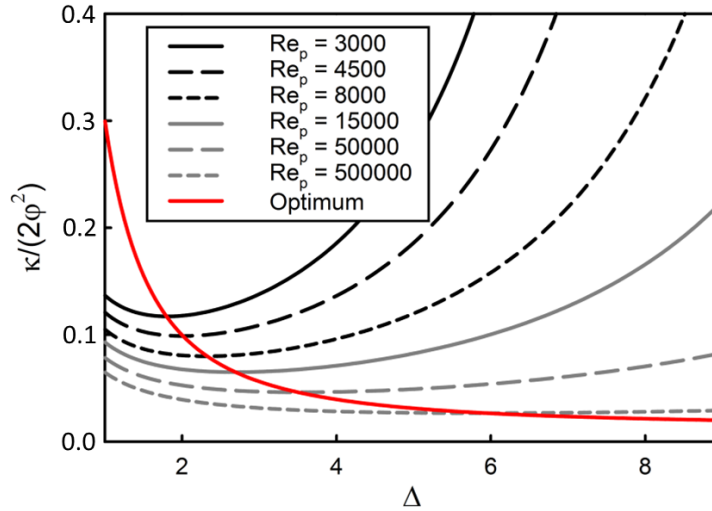


Figure 1 swirl atomizer design

In order to increase the spray angle and to obtain smaller drops, the intensity of the swirl inside the nozzle may be increased with modified nozzle geometries. However, the increased swirl intensity also affects the friction losses, which in case of low viscous liquids have minor effect on the atomizer performance. But, with increasing liquid viscosities, the energy losses become higher and at certain conditions, the sheet velocity decrease due to friction losses outweighs the increase in spray angle. This behavior can be shown with a plot of  $\kappa/(2\varphi^2)$  as a function of the swirl ratio  $\Delta$  for different Reynolds-numbers, as shown in Fig. 2. The Reynolds-number used here is the pressure based Reynolds-number  $Re_p$ , where the velocity is expressed with the atomization pressure and liquid density,  $v^2 = 2\Delta p/\rho_l$ :

$$Re_p = \frac{\sqrt{\rho_l \Delta p_l} D}{\mu_l} \quad (5)$$

For each  $Re_p$ -number, there is a certain swirl ratio  $\Delta$  indicating a minimum for the term  $\kappa(2\varphi^2)$ . According to eq. (1), the expected mean drop size becomes smallest at the same swirl ratio. For different  $Re_p$ -numbers, fig. 1 shows a shift of the optimal swirl ratio to higher  $Re_p$ -numbers. The reason for this behavior is the velocity coefficient, which decreases with higher swirl ratios. On the other hand the spray angle is increasing at the same time. This means that the optimal swirl ratio marks the compromise between the spray angle increase and the velocity coefficient decrease. For the case of very high  $Re_p$ -numbers, the friction losses can be neglected and therefore,  $\varphi$  becomes about 1 (not considering losses due to turbulence). Higher swirl ratio, i.e. higher swirl intensity then always mean smaller  $\kappa(2\varphi^2)$ -values and therefore smaller mean drop sizes.



**Figure 2** The course of  $\kappa(2\varphi^2)$  for different  $Re_p$ -numbers as function of the swirl ratio  $\Delta$ , including the track of the minimum, i.e. most favorable values  $\kappa(2\varphi^2)$

Another way to increase the spray angle and to decrease the drop sizes, apart from intensifying the swirl, is the application of swirl nozzles with Coanda deflection outlets [10]. Such orifices are also called trumpet shaped, as illustrated in figure 3, where  $R_C$  is the deflection radius. The deflection of the liquid sheet can be driven to spray angles up to 180 degrees, when  $R'_C = D/2 + R_C$ . Smaller spray angles are realized with  $R'_C < D/2 + R_C$ . However, the liquid sheet deflection is effective in a certain range of geometrical parameters and operating conditions only. As known from one-phase systems, too small deflection radii  $R_C$  lead to a premature detachment of the sheet, which is mostly unwanted. Although such nozzles are already part of the product line for most of the nozzle manufacturers, the description of the two-phase Coanda-effect is still sparse.

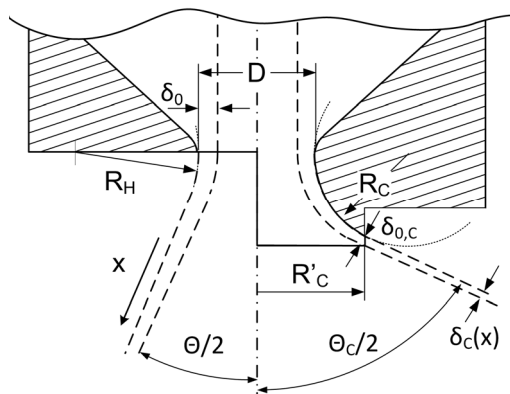


**Figure 3** left side: conventional swirl atomizer outlet (sharp edged), right side: Coanda-deflection outlet

### Coanda deflection at constant ambient gas pressure

The behavior of sheet deflections due to the Coanda-effect is analyzed by means of spray angle measurements at ambient pressure. Experiments at different  $Re_p$ -numbers and different nozzle geometries were performed. The spray angles were captured with a backlighting photography setup, which is further described in [9]. The  $Re_p$ -numbers were varied through the differential atomization pressure  $\Delta p$  and different liquid viscosities. The latter were achieved by mixing water and glycerol in certain ratios. The nozzle design used here is in ac-

cordance to the nozzle illustrated in Figure 1, with two tangential liquid inlets creating the swirl flow within the nozzle. Different swirl ratios  $\Delta$  (see equ. 4) are realized with a modular nozzle design, which was also used in the past [9]. In the present work, the nozzle outlet diameter is always  $D=6$  mm. As an example, results are shown in Figure 5. The left plot shows the spray angle course at different  $Re_p$ -numbers for various relative deflection radii  $R_c/D$  at constant swirl ratio of  $\Delta=0.96$ . The spray angle is nearly constant for the considered range of  $Re_p$ -numbers. The spray angle achieved without Coanda deflection,  $R_c/D=0$ , is around 75 degrees and there is a minor increase with increasing  $Re_p$ -numbers. When Coanda deflections are considered,  $R_c/D>0$ , the spray angle curves divide into two regions: a region where a proper deflection takes place and a region, where the Coanda radius  $R_c$  is obviously too small to deflect the sheet. In the operation range observed, the transition between the two regions is given with  $R_c/D=0.42$ . Following the spray angle course for  $R_c/D=0.42$ , there is a transition between proper deflection and preliminary detachment at  $Re_p$ -numbers around 60,000. According to these results, higher  $Re_p$ -numbers have a negative effect on the sheet deflection. For low  $Re$ -numbers, the film flow along the Coanda contour will follow the contour without detachment even at low deflection radii. At higher film Reynolds numbers the flow detaches, as is the case for the flow around a cylinder or a sphere under fully immersed conditions (single phase flow). The pressure along the streamlines close to the surface rises due to retardation within the boundary layer until the dynamic pressure is too low to overcome the local static pressure. Applied to the flow along a Coanda contour the spray angle is reduced when detachment takes place. Only at very high Reynolds numbers reattachment may occur as soon as the boundary layer flow becomes highly turbulent transporting more energy (see e.g. Schlichting [8]). Reattachment is also achieved by obstacles like trip wires even at lower  $Re$ -numbers forcing the laminar boundary layer to become turbulent earlier.

However, because the sheet velocity and the liquid viscosity are included in the  $Re_p$ -number, it is not possible to make statement whether both, or only one of these two parameters influences the deflection. For further analysis, the spray angles for different swirl ratios and various liquid viscosities are plotted in Figure 5 (right). In this case the atomization pressure is kept constant, but comparable sheet velocities are only achieved with viscosities up to  $\mu=10$  mPa. Higher liquid viscosities show a remarkable velocity decrease, because of the friction losses within the nozzle. Within the swirl ratio range covered in the right diagram of Figure 5, there is a minor increase of spray angle for increasing swirl ratios. Obviously, when the spray angle is increasing due to the intensified swirl flow, even higher spray angles are reached with Coanda deflection outlets. Furthermore, following the courses in Figure 5 right, lower spray angles are reached for increasing liquid viscosities and for both deflection radii  $R_c/D$ . Keeping this in mind and going back to the previous diagram, Figure 5 left, the transition seen for  $R_c/D=0.42$  seems to be mainly caused by the sheet velocity. On the other hand, none of these diagrams considers the influence of the sheet thickness, which is known to increase with increasing liquid viscosities [1]. A parameterization of the spray angle as a function of the influencing parameters including the sheet thickness may probably lead to better understanding of the Coanda deflection behavior. Also a sheet velocity measurement near the orifice could clarify the case. Such measurements are planned in the near future using invasive fiber-optical methods, as shown in [9].

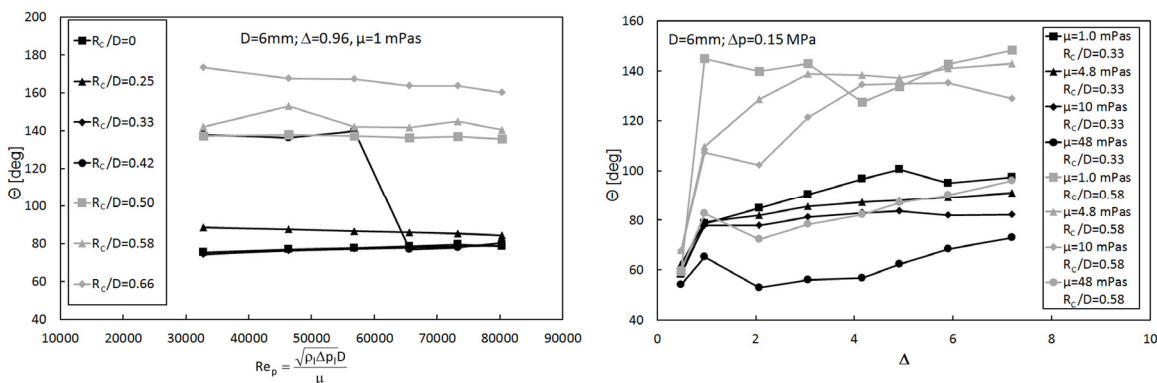


**Figure 5** left side: spray angle as function of the  $Re$ -number for different deflection radii and for  $\Delta=0.96$  and  $\mu=1$  mPas, right side: spray angle versus swirl ratio  $\Delta$  for different liquid viscosities and  $R_c/D= 0.33$  (black) and  $R_c/D= 0.58$  (grey)

However, the effect of liquid flows following a curved surface, as shown in Fig. 3, may also be linked to the “tea pot effect”. In fact, many authors don’t distinguish between the “Coanda-deflection” and the “tea pot effect”[7]. While the “tea pot effect” is strongly depending on the wetting angle, the Coanda-effect is linked to entrainment connected to under-pressure and the boundary layer interaction of fast flowing streams within a static environment. Because of the relatively high sheet velocities, even beyond 10 m/s for the most applications,

the influence of the wetting angle of contact is unlikely. Nevertheless, experiments were performed with different nozzle materials in order to uncover potential contact angle dependencies. One nozzle was made of hydrophilic aluminum (oxidized), with a very low contact angle ( $\Theta = 13^\circ$ ) to the fluid, and as an opposite, a polyvinylchloride nozzle with high contact angle ( $\Theta = 82^\circ$ ) was machined. Both deflection bodies were polished using sandpaper (10  $\mu\text{m}$  grit) and a polish suspension (1  $\mu\text{m}$  grit) in order to achieve a comparable surface smoothness. Pictures of the nozzle bodies are illustrated in Figure 4 (left). In Figure 4 (right) spray angles achieved with the Coanda nozzles are shown for  $\mu=10\text{ mPas}$  and different deflection radii. As already shown in the previous diagrams, the spray angle is increasing with increasing swirl ratios. Comparing the influence of the nozzle material, i.e. aluminum (grey) and PVC (black), it becomes obvious that there is no influence of the nozzle material on the deflection behavior. At least at the chosen operating conditions, the experimental results lead to the conclusion that contact angle effects are negligible and therefore, the “tea pot effect” is not significant for the sheet deflection.

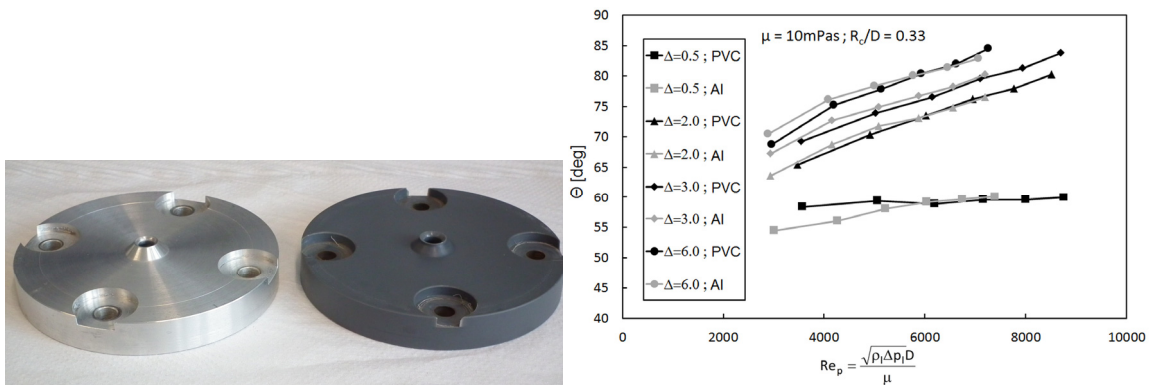


Figure 4 left side: picture of the nozzle bodies made of aluminum and PVC, right side: comparison of spray angles achieved with the aluminum (grey) and the PVC (black) nozzle

#### Spray angle measurements with variable ambient gas pressure

Deflecting a liquid film on a convex surface causes lower pressure at this surface. As the ambient pressure of the environmental atmosphere helps to hold the film in its place but simultaneously leads to disturbance of the gas-liquid interface at the air core, it was to be examined how the ambient atmosphere finally affects the flow at trumpet openings. For that purpose a nozzle was chosen in the following experiments with geometry sensitive to flow detachment, i.e. geometry with low swirl.

In order to analyze the influence of the ambient atmosphere on the sheet deflection, experiments were performed in a vessel (figure 6). The vessel is designed for over-/under-pressures of 3 and -1 bar respectively. Overpressures are realized through a pressurized air supply, while under-pressure was achieved with a turning head vacuum pump, allowing for pressures of 800 mbar below the atmospheric pressure. The sheet formed at the nozzle for given liquid overpressure could be observed through a sight glass and photos were taken from the spray angle with a camera.

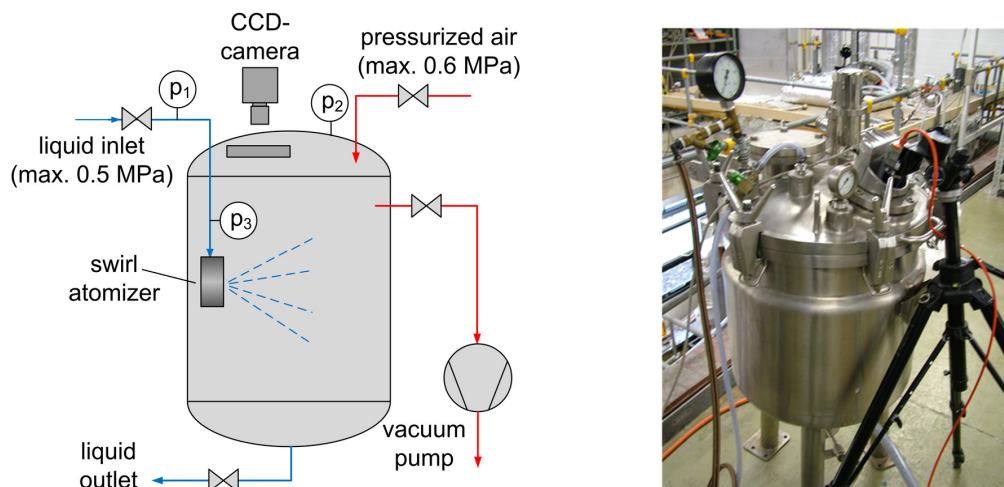
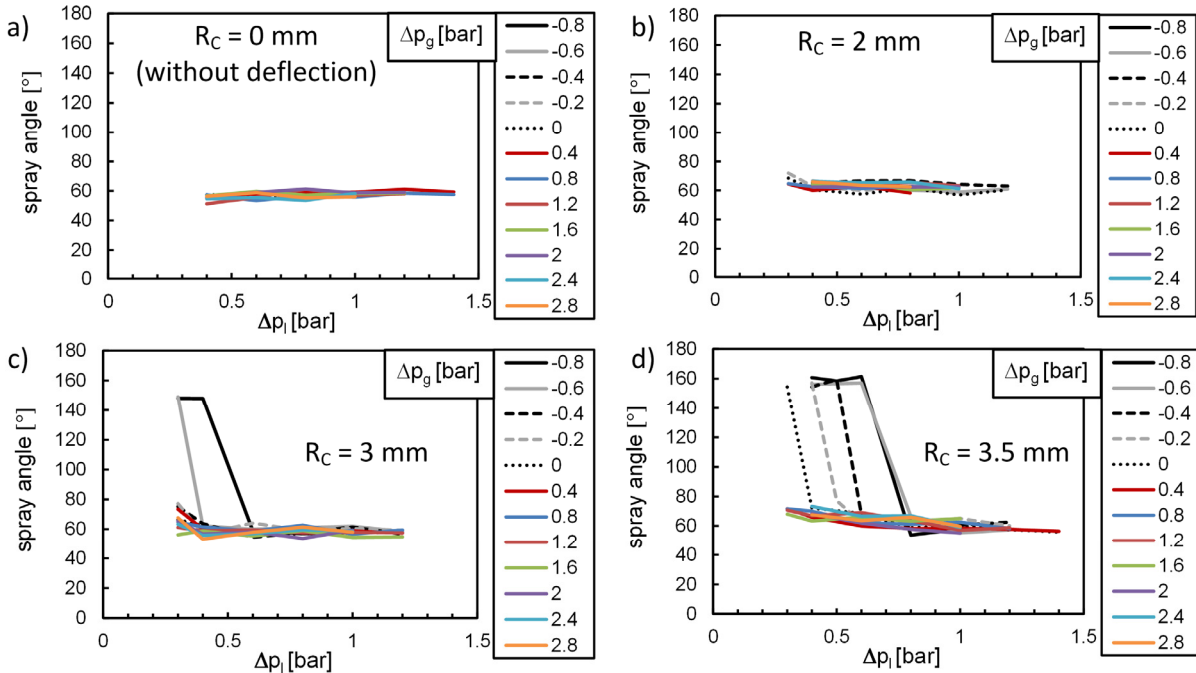


Figure 4 experimental setup for atomization at variable ambient pressures, right: photography of the pressure vessel.

The swirl nozzle is fixed at the vessel sidewall and therefore, the spray is propagating horizontally. For imaging of the spray formation near the nozzle outlet, a PCO Pixelfly CCD-camera was used, which is suitable for low exposure time photography rather than for high-speed imaging. The inspection glass was located at the top of the vessel and it also carried the light source. The whole internal surface of the vessel was covered with filter mats to prevent drop impact effects, which otherwise reduce the imaging quality due to drop deposition on the sight glass. As illustrated in figure 6, three pressure indicators were installed for controlling operating conditions. Indicators  $p_1$  and  $p_3$  indicate the pressure difference for the liquid flow in the line as ( $p_1$ ) is the overhead pressure of the liquid and ( $p_3$ ) is the liquid pressure close to the nozzle, ( $p_2$ ) indicates the gas (air) pressure within the vessel respectively. The pressure difference between indicators  $p_3$  and  $p_2$ , is the actual atomization pressure  $\Delta p_l$  which determines the discharge velocity of the liquid from the nozzle. The overpressure inside the vessel is defined as  $\Delta p_g = p_2 - p_0$ , where  $p_0$  is the atmospheric pressure.

The nozzles used here are significantly smaller with  $D = 6$  mm, than the nozzle of the previous experimental setup. In order to observe the limiting case for the critical  $R_C/D$ -ratio, indicating the transition from clearly visible Coanda deflection to premature sheet detachment with lower spray angle, different nozzles with different swirl ratios  $\Delta$  were tested. Finally, two nozzles were identified with the desired operating behaviour, one with  $R_C/D = 0.58$  and  $\Delta = 0.48$ , the other with  $R_C/D = 0.42$  and  $\Delta = 0.86$ .

These two nozzles were operated in the pressure vessel and their spray angles were documented by photographs with and without trumpet openings ( $R_C = 0$ ). The results for the first mentioned nozzle geometry are presented in figure 7. For the operation without Coanda deflection outlet ( $R_C = 0$ ), illustrated in figure 7a, the spray angle is around 60 degrees for all operating conditions, i.e. for all liquid side and gas side overpressures. Switching to a Coanda-orifice with  $R_C = 2$  mm, as shown in figure 7b, there is a slight increase in spray angle compared to  $R_C = 0$  mm. However, the effect can be neglected. The chosen deflection radius is obviously too small for the liquid to follow the deflection contour and premature detachment occurs.



**Figure 5** Spray angle for different liquid pressures  $\Delta p_l$ , various ambient gas pressures  $\Delta p_g$  and Coanda-deflection radii  $R_C$ , while the swirl ratio  $\Delta$  and the orifice diameter are kept constant at  $\Delta = 0.48$  and  $D = 6$  mm

Increasing the Coanda deflection radius to  $R_C = 3$  mm, it was observed, that at very low ambient gas pressures, between  $-0.6$  and  $-0.8$  bar, significantly higher spray angles are achieved even at same differential pressures of the liquid. Further increase of the deflection radius to  $R_C = 3.5$  mm expands the range of ambient gas pressures to  $-0.8 \leq \Delta p_g \leq 0$  bar. In this range now the spray angles are considerably increased at given liquid differential pressures, i.e. at given flow velocities of the liquid. These experiments clearly indicate that there is a visible influence of the ambient gas pressure on the deflection and detachment behavior of the liquid at trumpet openings.

For visualization of the emerging sheet at different ambient gas pressures, images of the spray structure are shown in figure 8. Here, a deflection with  $R_C/D = 3$  mm and a constant liquid overpressure of  $\Delta p_l = 0.4$  bar corresponding to identical flow rates are chosen. The corresponding spray angle plot for this nozzle is illustrated in

figure 7c. The plot shows that at low ambient gas pressures, e.g. at  $\Delta p_g = -0.8$  bar, a wide spray angle is achieved and the spray hits the inspection glass of the vessel. For  $\Delta p_g = 0$  bar, the sheet detaches from the orifice like there was no deflection at all despite of the mounted trumpet. For higher ambient gas pressures, at  $\Delta p_g = 2.8$  bar, there is no significant change in spray angle, but the location of sheet break up moves towards the orifice, as the aerodynamic stimulation is intensified due to the higher gas density.

In the following, possible explanations for this behavior are discussed. The Reynolds number defined by the differential pressure of the liquid determines the flow conditions within the film at a given geometry. The liquid sheet inside the nozzle has permanent contact with the nozzle wall, where the no-slip condition for viscous fluids requires that the fluid has zero velocity close to the wall. At the air core there is a boundary layer to the gas and a continuous entrainment and reflux of the gas causes a loss of predominantly angular and with increasing radial location also radial momentum in the film flow. This momentum loss is stronger in case of higher gas densities and may lead to earlier detachment from the trumpet contour.

At the location, where the liquid sheet detaches from the nozzle wall, a new boundary layer within the gas phase is formed close to the sheet surface. The environmental gas has to be accelerated along with the moving film, which means a pressure increase in the liquid phase with earlier detachment in case of higher gas density.

$\Delta p_g = -0.8$  bar ( $p_g = 0.2$  bar abs.)



$\Delta p_g = 0.0$  bar ( $p_g = 1.0$  bar abs.)



$\Delta p_g = 2.8$  bar ( $p_g = 3.8$  bar abs.)

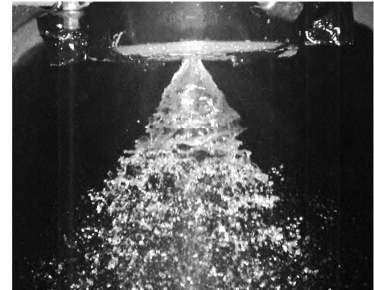


**Figure 6** Shape of the emerging sheet at different ambient gas pressures, but constant atomization pressure of  $\Delta p_l = 0.4$  bar corresponding to constant flow rate and a atomizer geometry with  $R_c/D = 0.58$  and  $\Delta = 0.48$

However, one should consider that the observed behavior only exists at the fairly low overhead pressure and only represents a small range of typical spraying conditions. At the detachment location with zero velocity boundary condition at the wall, it is assumed that the velocity profile has a turning point close to the surface as in a diffuser with flow detachment. As the boundary layer moves with the sheet, gas is transported away from the detachment location, which causes a local pressure drop. The entrained surrounding gas compensates the pressure decay. But as soon as the gap between the nozzle wall and the liquid sheet becomes too tight, the inflowing gas is not anymore able to balance the pressure drop as a considerable amount of gas is transported along with the rough liquid surface. It is obvious that higher gas densities due to intensified momentum transfer promote earlier detachment. The turbulent structure of the liquid flow as well as the sheet thickness surely also strongly influences the detachment behavior. The detached region of the sheet frequently shows a strongly disturbed, i.e. rough surface. Furthermore, the system is three-dimensional and therefore difficult to capture and to analyze.

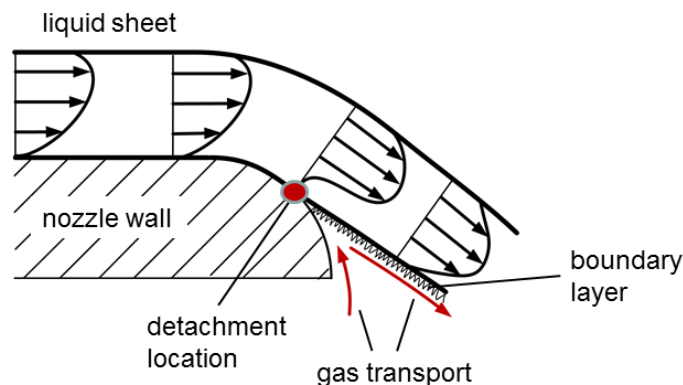


**Figure 7** principle of liquid sheet detachment at Coanda deflection nozzles

## Summary and Conclusions

In the present work, the basic behavior of swirl nozzles with simple sharp edged openings is described first. Based on simple generally recognized estimation methods for the mean drop size, it can be found that there is an optimum in swirl numbers for smallest droplets at given differential pressure according to the specified running conditions and liquid properties. High swirl reduces the sheet thickness but leads to higher energy loss. Coanda or trumpet openings unlock an additional optimization design as large spray angles can also be achieved with low swirl but subsequent deflection of the sheet. The flow of the sheet along Coanda contours is complex and still has to be analyzed in detail. Detachment conditions were discussed but so far not yet described by a closed theory. It was observed, that higher Reynolds-numbers lead to an earlier sheet detachment. The wetting angle of the nozzle material was found to have no influence on the deflection behavior, indicating that the “tea pot effect” is not significant within the considered operational area. Experiments were able to show that at fairly low discharge velocities of the liquid even the ambient gas pressure influences the usually unwanted detachment behavior of the sheet from the deflection contour. Extensive examinations are still needed to quantitatively describe detachment behavior, energy loss and sheet thickness increase at Coanda-deflection outlets and to include this nozzle design into optimizing procedures.

## Acknowledgements

The authors want to express their gratitude to the German research foundation „Deutsche Forschungsgemeinschaft (DFG)“ for their financial support of the project.

## Nomenclature

symbol	description	unit
$A_D$	discharge cross section	m <sup>2</sup>
$D$	nozzle orifice diameter	m
$p$	absolute pressure	MPa, bar
$\Delta p$	pressure gradient	MPa, bar
$\Delta p^* = \Delta p \delta / \sigma$	nozzle Laplace-number	-
$R_C$	Coanda deflection radius	m
$R'_C$	Coanda detachment radius	m
$r_{SC,E}$	entry swirl chamber radius	m
SMD	Sauter mean diameter	m
$u$	tangential velocity	m/s
$\dot{V}$	volumetric flow rate	m <sup>3</sup> /s
$v$	axial velocity	m/s
$\bar{v} = \dot{V} / A_D$	mean axial velocity	m/s
$w$	sheet velocity	m/s
$x$	sheet running length	m
$\delta$	sheet thickness	m
$\Theta$	spray angle	deg.
$\mu$	dynamic viscosity	kg/(m·s)
$\rho$	density	kg/m <sup>3</sup>
$\sigma$	surface tension	kg/s <sup>2</sup>

## References

- [1] Lefebvre, A.H., *Atomization and Sprays*, Taylor & Francis, Oxford (1988)
- [2] Dombrowski, N., Johns, W.R., *Chemical Engineering Science* 18-3: 203 (1963)
- [3] Senecal, P.K., Schmidt, D.P., Nouar, I., Rutland, C.J., Reitz, R.D., Corradini, M.L., *International Journal of Multiphase Flow* 25-6-7: 1073 (1999)
- [4] Musemic, E., Gaspar, M., Weichert, F., Müller, H., Walzel, P., *ILASS 2012*, Brno, Czech Republic, Sep. 6-8 (2010)
- [5] Musemic, E., Walzel, P., *Chem. Ing. Tech.* 83-3: 237 (2011)
- [6] Walzel, P., *Ullmann's Encyclopedia of Industrial Chemistry, Spraying and Atomizing of Liquids*, Wiley-VCH (2010)
- [7] Lubert, C., *Int. J. of Acoustics and Vibrations*, 16-3:144-153 (2011)
- [8] Schlichting H, Gersten K, *Grenzschicht-Theorie*, Springer Berlin / Heidelberg, Heidelberg (2006)
- [9] Musemic, E., Walzel, P., Gaspar, M., Weichert, F., *ILASS 2008*, Como Lake, Italy, Sep. 8-10 (2008)
- [10] Dusy, M., *diploma thesis*, Univerität Essen, Essen, Germany (1988)